Effects of Precipitation Uncertainty on Discharge Calculations for Main River Basins

H. BIEMANS

Earth System Science and Climate Change, Wageningen University and Research Centre, Wageningen, and Netherlands Environmental Assessment Agency, Bilthoven, Netherlands

R. W. A. HUTJES AND P. KABAT

Earth System Science and Climate Change, Wageningen University and Research Centre, Wageningen, Netherlands

B. J. STRENGERS

Netherlands Environmental Assessment Agency, Bilthoven, Netherlands

D. GERTEN AND S. ROST

Potsdam Institute for Climate Impact Research, Potsdam, Germany

(Manuscript received 23 June 2008, in final form 20 November 2008)

ABSTRACT

This study quantifies the uncertainty in discharge calculations caused by uncertainty in precipitation input for 294 river basins worldwide. Seven global gridded precipitation datasets are compared at river basin scale in terms of mean annual and seasonal precipitation. The representation of seasonality is similar in all datasets, but the uncertainty in mean annual precipitation is large, especially in mountainous, arctic, and small basins. The average precipitation uncertainty in a basin is 30%, but there are strong differences between basins. The effect of this precipitation uncertainty on mean annual and seasonal discharge was assessed using the uncalibrated dynamic global vegetation and hydrology model Lund–Potsdam–Jena managed land (LPJmL), yielding even larger uncertainties in discharge (average 90%). For 95 basins (out of 213 basins for which measurements were available) calibration of model parameters is problematic because the observed discharge falls within the uncertainty of the simulated discharge. A method is presented to account for precipitation uncertainty in discharge simulations.

1. Introduction

There is a growing concern about increasing water scarcity in many regions of the world, as climate change on the one hand and increasing human water use on the other can put increasing pressure on the world's water resources (CSD 1997; Kundzewicz et al. 2007; World Water Council 2000).

Understanding the processes leading to (repetitive) droughts and floods requires an extensive understanding of the global hydrological cycle and its interactions with vegetation, climate, and humans (Kabat et al. 2004). Not only should average annual water availability be quantified with certainty but also the spatial and temporal distribution of water availability. There are several studies that calculate soil moisture, runoff, and its accumulation in discharge based on climate input, soil, and vegetation characteristics using global-scale hydrological models (e.g., Alcamo et al. 2003; Arnell 1999b; Gerten et al. 2004; Nijssen et al. 2001; Oki et al. 2001; Vörösmarty et al. 1998). Most of these models have been used to simulate current discharge patterns, but a number of global assessments on the influence of climate change on future water resources exist (e.g., Alcamo et al. 2007; Arnell 1999a, 2003; Barnett et al. 2005; Bergström et al. 2001; Milly et al. 2005; Vörösmarty et al. 2000a).

For a reliable quantitative assessment of future water resources, it is important to first gain trust in the

Corresponding author address: H. Biemans, Earth System Science and Climate Change, Wageningen University and Research Centre, P.O. Box 47, Wageningen 6700 AA, Netherlands.
E-mail: hester.biemans@wur.nl

DOI: 10.1175/2008JHM1067.1

simulation of current water availability. This can be done by validating the global model to observed discharges, for which data are available globally (Global Runoff Data Centre 2007). Discharge is the integrator of the water balance over large areas and can be regarded as the water availability in different sectors.

Few global hydrological models have been validated and calibrated to discharge observations so as to reduce the bias between observations and simulations. This was done by adjusting the model parameters (Nijssen et al. 2001) or by applying a simple correction parameter (Döll et al. 2003). However, the bias between observations and simulations cannot always be attributed to the model designs. If, for example, the precipitation input data in a particular basin is too low, it is logical that the simulated streamflow becomes too low, even though the parameterization of the runoff generation process may be physically correct. Tuning the model to observed discharge can thus result in a compensation of the underestimated or overestimated precipitation, leading to an unrealistic partitioning of precipitation between runoff and other water balance terms. Therefore, the uncertainty in model simulations arising from different factors should be taken into account before calibrating the model parameters.

Wind-induced undercatch of solid precipitation (Adam and Lettenmaier 2003) and underestimation of precipitation in topographically complex regions (Adam et al. 2006) are well-known sources of errors in precipitation products derived from rain gauge measurements. Tian et al. (2007) compared water balance calculations with undercatch-corrected and uncorrected precipitation data and demonstrated that using bias-corrected precipitation resulted in an increase in computed streamflow of 5%–25% in northern latitudes.

The question of which precipitation dataset is the most accurate for forcing of hydrological models is posed in several studies, but has not yet been answered with consensus. Berezovskaya et al. (2004) showed inconsistencies between runoff data and three precipitation datasets for three large Siberian rivers. Their analysis suggests a poor quality of either the runoff or precipitation datasets, or both. Pavelsky and Smith (2006) used discharge observations of 198 arctic rivers to assess the quality of four global precipitation sets and concluded that observational datasets cover the trends significantly better than two reanalysis products. At global scale, however, Voisin et al. (2008) evaluated a reanalysis precipitation product more suitable than a satellite-derived precipitation dataset for use in a hydrological model, mainly because of the high temporal resolution of the reanalysis product.

Fekete et al. (2004) demonstrated the impact of uncertainties in precipitation input on runoff estimates at a grid scale by forcing a global water balance model with six different global precipitation datasets. This analysis showed that the uncertainty in precipitation translates to at least the same and typically much greater uncertainty in runoff in relative terms. Although the sources of the differences between the datasets were not identified, the Fekete et al. (2004) study demonstrated the importance of taking a close look at the climate input data that is used to force the hydrological model. However, they did not compare the datasets on a basin scale, which is the common scale for water resources assessments. The problem of uncertainties in input data for global hydrological models and the resulting over- or underestimations of streamflow in several basins has been identified in several papers (e.g., Döll et al. 2003; Gerten et al. 2004; Nijssen et al. 2001), but its individual contribution to overall uncertainty has, to our knowledge, not yet been quantified at global scale. Although there are possible uncertainties in all input datasets (e.g., soil, land use, temperature), in this paper we will focus on the impact of uncertainty in precipitation data, which we expect to be the largest source of uncertainty from input data.

For water resources assessments, the intra-annual dynamics of discharge are important, because both water demand and supply vary throughout the year. Therefore, the impact of uncertainty should also be investigated on a seasonal time scale.

The objective of this paper is to quantify the global distribution of the uncertainty in annual as well as seasonal estimates of precipitation on a basin scale and the resulting uncertainty in discharge estimates as computed by the Lund–Potsdam–Jena managed land (LPJmL) model (Bondeau et al. 2007; Rost et al. 2008). Based on the results, consequences of this uncertainty for validation and calibration of global hydrological models are discussed. Specifically, we compare the variations between seven global gridded precipitation datasets at a basin scale, analyze the simulated variations in discharge on a mean annual and a mean seasonal time scale, and compare the outcomes with observations for 294 basins around the world. More detailed analyses are presented for a selection of 16 basins located in different climate zones and with different hydrological properties. The analysis for all 294 basins is available in an online database (http://www.climatexchange.nl/projects/JHM).

Section 2 gives an overview of the method: the seven global precipitation datasets used, other input data for the LPJmL model, a brief model description, and the data used for validation. In section 3 the results of the

TABLE 1. Main characteristics of the seven global gridded precipitation sets used in this study. Extensive analyses of seven precipitation datasets, calculated discharge accounting for the precipitation uncertainty, and comparisons with station observations for all 294 basins is available in an online database (http://www.climatexchange.nl/projects/JHM).

Dataset	Resolution	Period	Source	Description
CRU	0.5	1901–2002	http://www.cru.uea.ac.uk/cru/data/hrg.htm	New et al. (1999, 2000)
CRU–PIK	0.5	1901–2003	Potsdam-Institut für Klimafolgenforschung http://www.pik-potsdam.de/	Österle et al. (2003)
MW	0.5	1900–2006	http://climate.geog.udel.edu/~climate/	Matsuura and Willmott (2007)
GPCC	0.5	1951–2000	http://www.dwd.de	Beck et al. (2005)
GPCP	2.5	1979–2007	http://cics.umd.edu/~yin/GPCP/main.html	Adler et al. (2003)
CMAP	2.5	1979–2007	http://www.cpc.ncep.noaa.gov/products/global_precip/html/wpage.cmap.html	Climate Prediction Center (2007)
ADAM	0.5	1979–99	http://www.ce.washington.edu/~jenny/global_sim.html	Adam et al. (2006)

analysis are presented in three parts: (i) the precipitation uncertainty, (ii) the impacts of this uncertainty on discharge simulations, and (iii) comparison with observed discharge. Section 4 discusses the implications of these results for validating, developing, and calibrating global hydrological models and concludes with the representation of uncertainty in modeling results.

2. Method and data

a. Precipitation input

In this study we use seven global gridded precipitation sets (Table 1) and compare them at basin scale. These datasets differ with respect to the original data sources that are used, the interpolation method, and the eventual correction factors applied. The datasets are selected based on their spatial coverage (global) and their temporal coverage (at least a 20-yr time series).

The Climate Research Unit (CRU) of the University of East Anglia developed the CRU dataset. It consists of a climatology (New et al. 1999) and monthly anomalies to this climatology (New et al. 2000) at a global 0.5° resolution, of which monthly values for precipitation, temperature, cloud cover, and number of wet days per month are used for the present study. The dataset has recently been updated (CRU TS 2.1) (Mitchell and Jones 2005) for the years 1901–2002. CRU is chosen as our reference dataset because it provides a full forcing dataset to run the model (precipitation, temperature, number of wet days, and cloud cover).

Österle et al. (2003) showed that the time series of temperature and precipitation in the first CRU database that covers the period 1901–98 (New et al. 2000) were corrupted with inhomogeneities. These inhomogeneities were adapted for each grid cell using a correction procedure (Österle et al. 2003). To extend the data to 1999–2003, an earlier version of the Global Precipitation Climatology Centre (GPCC) data (described below) for each $1° \times 1°$ grid cell was used and interpolated onto a 0.5° grid based on the correlations between the grid cells derived from the original CRU precipitation data between 1986 and 1998. The precipitation dataset that has been developed by Österle et al. (2003) is referred to herein as CRU–Potsdam–Institut für Klimafolgenforschung (CRU–PIK).

The global precipitation dataset (MW), developed by Matsuura and Willmott (2007), covers the period 1900–2006 and comprises monthly time series at 0.5° resolution. This precipitation dataset is based only on station data from several sources. Station climatology from the Legates and Willmott (1990) unadjusted (for rain gauge undercatch) archive were used as a part of the background climatology. Station precipitation values were not adjusted to reduce rain gauge undercatch bias. The stations were not checked for temporal heterogeneities because the main goal of this dataset was to represent spatial patterns of rainfall rather than homogenous time series.

The most recent version of the GPCC global precipitation dataset (Beck et al. 2005) consists of monthly precipitation fields on a 0.5° grid for the period 1951–2000. The dataset is based only on station observations that have met high demands concerning the quality and temporal coverage; therefore, this dataset is mainly suitable to study temporal variability. Interpolation has been done using ordinary kriging.

The Global Precipitation Climatology Project (GPCP), which is a part of the Global Energy and Water Cycle Experiment (GEWEX), developed a monthly precipitation dataset for 1979–2003 (Adler et al. 2003). The resolution of this dataset is 2.5°. It is based on a previous version described by Huffman et al. (1997) and was derived by merging satellite and surface rain gauge data. The gauge data have been corrected for systematic errors using a monthly correction factor as derived by Legates (1987).

The Climate Prediction Center Merged Analysis of Precipitation (CMAP) is a dataset that comprises both pentad and monthly analyses of global precipitation (Climate Prediction Center 2008; Xie and Arkin 1997). Observations from rain gauges were merged with precipitation estimates from several satellite-based algorithms (infrared and microwave). The analyses were performed on a 2.5° grid and extend back to 1979. The dataset with monthly values is used here.

The global precipitation dataset developed by Adam et al. (2006) (ADAM) is based on a previous version of the Matsuura and Willmott database (Willmott and Matsuura 2001). This dataset has been adjusted to correct for systematic wind-induced undercatch and wetting losses from rain gauges (Adam and Lettenmaier 2003) as well as for orographic effects (Adam et al. 2006). The combination of both adjustments resulted in a net increase of 17.9% in global land precipitation, as compared to Willmott and Matsuura (2001). The monthly data is available on a 0.5° grid for 1979–99.

First, the precipitation datasets are analyzed. For each basin determined by the validation stations (described in section 2c), the mean annual precipitation for the overlapping period 1979–99 is derived for all seven precipitation datasets:

$$P_{s,b} = \frac{1}{21} A_b^{-1} \sum_{y=1979}^{1999} \sum_{m=1}^{12} \sum_{c=1}^{n} P_{s,c,m,y} A_c, \qquad (1)$$

where $P_{s,c,m,y}$ is the precipitation in dataset s, cell c, month m, and year y; A_c is the area of cell c, A_b is the area of the basin b, and n is the selection of cells that fall within the basin b. The GPCP and CMAP data are only available onto a 2.5° grid but were projected onto a 0.5° grid. No interpolation method was applied, but each 2.5° grid cell was divided in 25 grid cells of 0.5° with the same values.

The maximum mean annual precipitation per basin b is determined by

$$P_{\max,b} = \max(P_{1,b}, \cdots, P_{7,b}), \qquad (2)$$

and the minimum mean annual precipitation is derived analogously.

The absolute range in precipitation, representing the absolute uncertainty, is then given for each basin by

$$\Delta P_{\text{abs},b} = P_{\max,b} - P_{\min,b}. \qquad (3)$$

The relative range in precipitation, which is representing the relative uncertainty in precipitation, is given by

$$\Delta P_{\text{rel},b} = 100 \frac{P_{\max,b} - P_{\min,b}}{P_{\text{cru},b}}. \qquad (4)$$

The area-weighted relative uncertainty is calculated as

$$\Delta P_{\text{rel,weightedavg}} = \sum_{b=1}^{294} (\Delta P_{\text{rel},b} A_b) \Big/ \sum_{b=1}^{294} A_b. \qquad (5)$$

Subsequently the minimum and maximum of the mean annual precipitation calculations per basin are used to create the models' precipitation forcing. This is done by using the minimum and maximum values calculated in Eq. (2), multiplied by the original CRU data for all basins:

$$P_{\max,c,m,y} = \frac{P_{\max,b}}{P_{\text{cru},b}} P_{\text{cru},c,m,y}. \qquad (6)$$

The minimum precipitation forcing $P_{\text{minc},m,y}$ was created analogously.

Thus, this created input data that covers the range in precipitation estimates per basin but retains the spatial and temporal pattern of CRU. Two model runs were made to determine the resulting minimum and maximum simulated discharge for each basin.

For the uncertainty in seasonality of precipitation the same procedure was followed: for each precipitation dataset the mean seasonal [December–February (DJF), March–May (MAM), June–August (JJA), and September–November (SON)] precipitation for 1979–99 was derived for each basin. The minimum and maximum of those seasonal totals were used to scale the respective seasons of the CRU dataset.

It is not our aim to give a quality judgment on the precipitation data in this study. Therefore, the seven precipitation sets are all given equal weight, and the range of precipitation values derived from these sets is assumed to represent the uncertainty in precipitation.

Note that LPJmL is a dynamic vegetation model (see section 2d) in which the spatial pattern of vegetation is closely linked to that of precipitation. To initialize the carbon and water pools, the model has been spun up for 1000 years by repeating the CRU climate of 1901–30 before the transient simulations (refer to Sitch et al. 2003). To prevent differences in simulated discharge between the runs from arising due to factors other than precipitation (e.g., the changed vegetation), we kept the spatial pattern of CRU and only used the precipitation totals derived from the other datasets.

b. Other climate input

Other meteorological variables used to force the model are monthly temperatures, the number of wet days per month, and the average monthly cloud fraction per grid cell so as to calculate potential evapotranspiration. These variables are all taken from the CRU

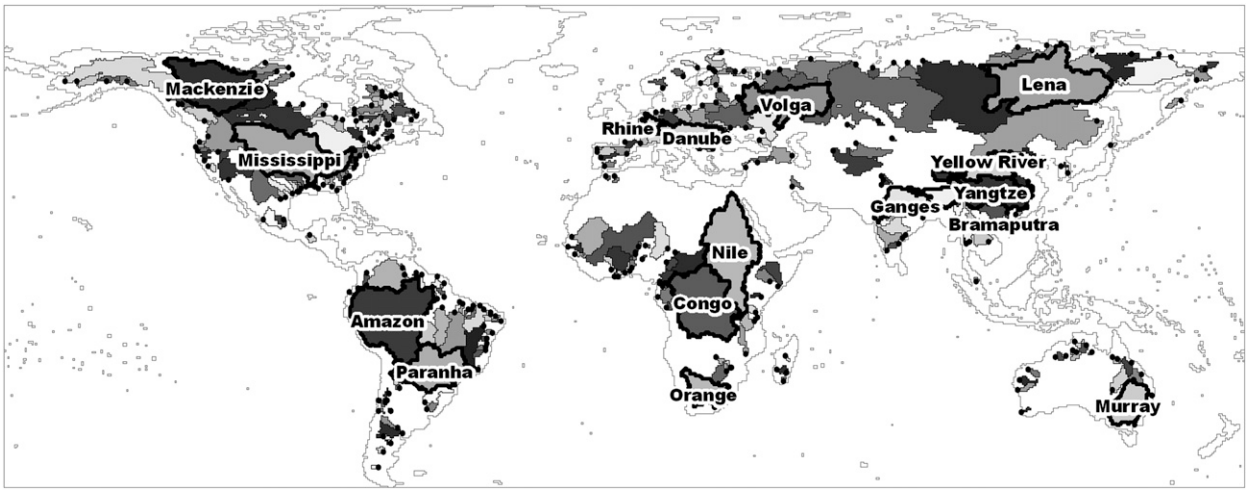

FIG. 1. Discharge stations used for validation and corresponding upstream areas.

database (Mitchell and Jones 2005; New et al. 1999, 2000) and are used for all simulations in this study.

c. Validation basins and data

There are several global gridded drainage direction maps (Döll and Lehner 2002; USGS 2000; Vörösmarty et al. 2000b). To compare the modeled discharge with the observations in a basin, it is important that the contributing area reported by the discharge measuring station matches the contributing area upstream of the station as calculated by the river network. We, therefore, use the Simulated Tropical Network at 30-min spatial resolution (STN-30p) (Vörösmarty et al. 2000b) for the accumulation and routing of computed runoff and a subset of 663 discharge stations that were co-registered to this network (Fekete et al. 2000, 2002). From these, we have analyzed the 294 most downstream stations of nested basins (Fig. 1: four basins were eliminated because their gauges fell outside of the LPJmL land mask). The area covered by these stations is approximately 70% of the world's actively discharging area (Fekete et al. 2002).

The 213 basins for which observation data are available (Global Runoff Data Centre 2007) for at least 5 years within the 1979–99 period are used to validate the model results with measured data.

d. Model description

We use the LPJmL dynamic global vegetation and water balance model (Bondeau et al. 2007; Gerten et al. 2004; Rost et al. 2008; Sitch et al. 2003) for the discharge simulations. LPJmL accounts explicitly for ecosystem processes such as the establishment, growth, and mortality of potential natural vegetation. In contrast to global hydrological models, it does not use a prescribed natural vegetation pattern but it dynamically computes (changes in) natural vegetation patterns from soil properties and climate. The vegetation competes for resources (water and light). The model calculates the full carbon and water balances, which are coupled, for example, through photosynthesis.

The LPJmL model uses a two-layered soil with a top layer of 0.5 m and a lower layer of 1 m thickness. The soil water balance is calculated daily, including precipitation, snowmelt, interception loss, soil evaporation, transpiration, percolation, and runoff. The total runoff is calculated as the sum of surface runoff from the top soil layer, subsurface runoff from the lower soil layer, and water percolating down through the lower soil layer. The surface and subsurface runoff are defined as the excess water above field capacity of the top and lower soil layers. Subsequently the runoff water is routed through the above-described gridded network with a constant velocity of 1 m s^{-1}.

Gerten et al. (2004) evaluated the water balance of an earlier version of the model for a small set of basins and concluded that the model results for runoff and evapotranspiration agree well with the results reported by state-of-the-art global hydrological models. However, all models in that analysis showed systematic bias in many regions, for example, an overestimation in dry regions and an underestimation especially in high latitudes. Recently, LPJmL has been extended with a representation of prescribed agricultural land (Bondeau et al. 2007) as well as a routing (including lakes) and irrigation scheme (Rost et al. 2008). This latter version is used here, although the irrigation module was switched off.

3. Results

a. Precipitation

1) Mean annual precipitation

At the global scale the seven precipitation datasets differ considerably in their global totals, although their interannual variability is largely similar (Fig. 2). The ADAM dataset gives substantially higher total land precipitation than the others, followed by GPCP. This can be explained by the application of correction factors for high elevation and snow-dominated areas in these datasets. The mean annual land precipitation estimates vary from 96 286 to 118 006 $km^3\ yr^{-1}$ (743–926 mm yr^{-1}) for the years 1979–99.

2) Mean annual precipitation per basin

Figure 3 shows the CRU mean annual precipitation as well as the relative range between the seven datasets for all basins [as Eq. (4)]. Although the largest absolute ranges can be seen in basins that have high precipitation (not shown), it is obvious from Fig. 3b that the largest relative ranges between the precipitation sets are found in mountainous and arctic regions and small catchments. This large uncertainty in precipitation in mountainous and arctic regions can be explained by the correction factors that have been applied in some datasets (ADAM and GPCP). The relative large ranges in small basins might be caused by the fact that variations between the datasets in the spatial distributions of precipitation are relatively more important for small basins, where it can be essential whether precipitation falls in a particular cell or a neighboring cell outside of the basin. In larger basins, those differences are more likely to average out over the total area. The weighted average precipitation range [Eq. (5)] per basin is 30%.

3) Seasonality in precipitation per basin

The absolute ranges in precipitation [derived as in Eq. (3) but with mean seasonal precipitation] per basin were found to be season dependent and to occur mainly in the wettest seasons (figure not shown). The mountainous arctic regions and small basins again show the largest relative ranges in precipitation in all seasons. Furthermore, the relative ranges in precipitation are largest in the Nordic basins (in the United States, Canada, Russia, northern Europe, and northern China) in winter. This is as expected because in this season most precipitation falls as snow, which is more difficult to measure (Adam et al. 2006). In ADAM and GPCP, a snow undercatch correction has been applied, which additionally explains the large variation among the different datasets. In summer the relative ranges are lower in those basins. For the other basins, the relative ranges in precipitation are more or less constant throughout the year.

Figure 4 presents the ranges in mean monthly precipitation for 16 basins (see locations in Fig. 1). It can be concluded from these graphs, as well as for the other 278 basins not shown here, that the differences between the precipitation datasets are caused by a relative shift in total precipitation. The patterns of monthly precipitation distribution are similar. [See also the online database for all other basins (http://www.climatexchange.nl/projects/JHM)]. There are no datasets that report the same mean annual precipitation values but do show a completely different distribution throughout the year. This can probably be explained by the fact that all datasets are partly based on the same station data, and the differences are caused by the interpolation and correction method applied and the additional sources used. The bias between the datasets cannot be traced back to one particular season, except for the basins where an undercatch correction has been performed. These basins show a relative higher precipitation uncertainty in the winter season compared to other seasons (e.g., in the Mackenzie and Volga river basins).

b. Discharge

1) Mean annual discharge per basin

The mean annual discharge simulated by LPJmL forced with CRU precipitation is shown in Fig. 6a. From Figs. 5 and 6b, it is clear that ranges in precipitation (Fig. 3) translate into similar patterns of ranges in discharge but with higher relative numbers (cf. Fig. 3b with Fig. 6b). Large uncertainties in discharge can be seen in the northern basins in Europe, Asia, and North America and in the mountainous regions and small basins. The area-weighted average uncertainty [as Eq. (5) but with discharge values] in the mean annual discharge calculations is 90% and thus is three times higher than the average uncertainty in precipitation.

Figures 6c and 6d illustrate the basin sensitivity to precipitation uncertainty. Figure 6c shows the fraction of precipitation uncertainty that results in runoff uncertainty. In regions where this fraction is high, the absolute uncertainty in discharge is almost the same as the absolute uncertainty in precipitation. Physically this means that in those areas the evaporative demand is largely met and the soil is very moist, causing extra precipitation to add to runoff immediately. Basins in the tropics and in high latitudes show a higher fraction than basins in temperate regions.

In relative terms, however, for almost all basins the relative discharge uncertainty is larger than the relative uncertainty in precipitation (if sensitivity >1 in Fig. 6d). This implies that the relative precipitation uncertainty is amplified in the discharge calculations.

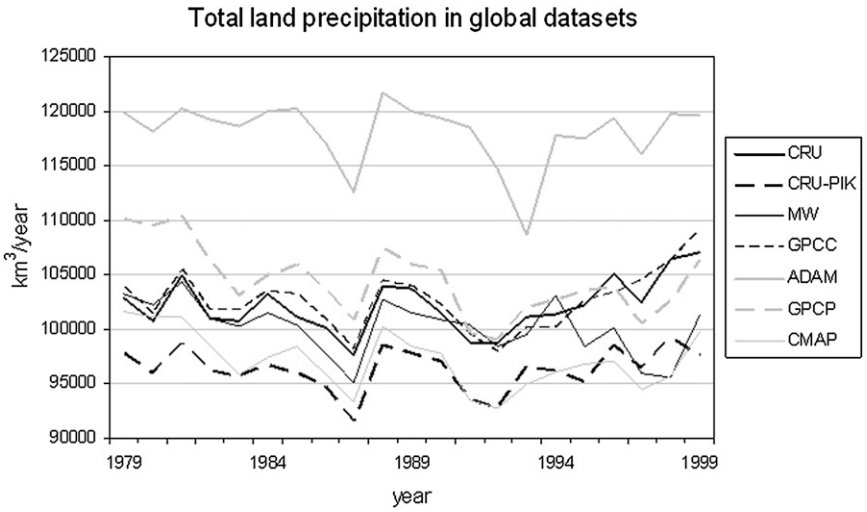

FIG. 2. Total land precipitation ($km^3\ yr^{-1}$) per year for seven global precipitation sets, 1979–99. Only cells common in the seven sets are taken into account.

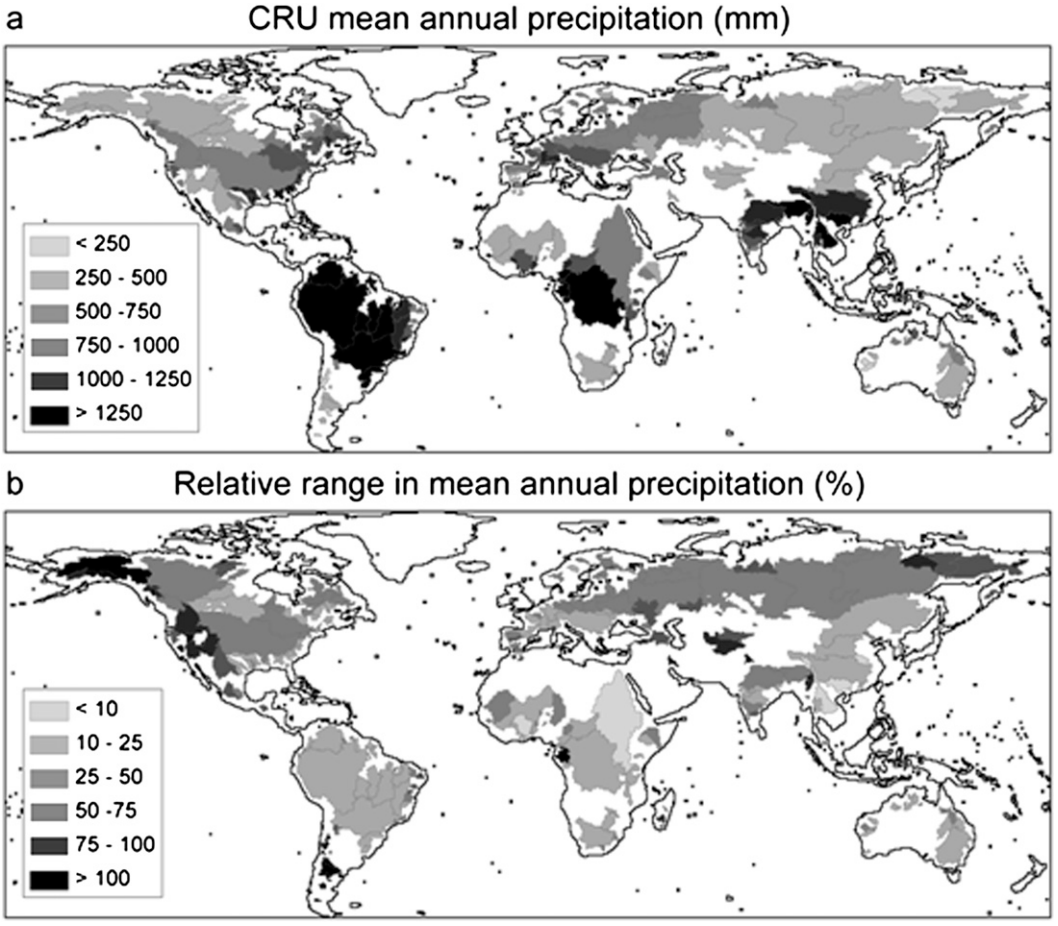

FIG. 3. (a) CRU mean annual precipitation per basin (mm $year^{-1}$) (1979–99) and (b) the range in mean annual precipitation between the seven datasets per basin as a percentage of the CRU mean annual precipitation.

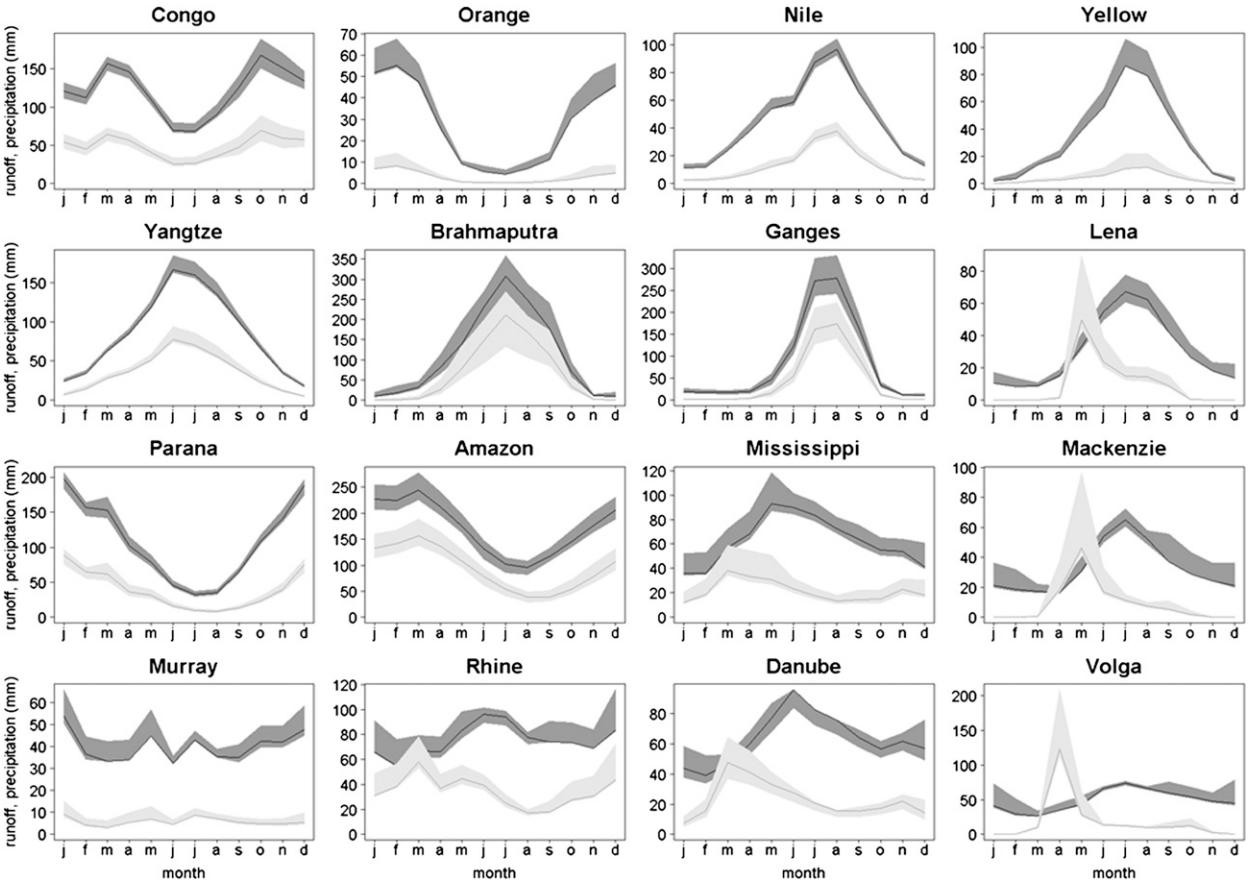

FIG. 4. Uncertainty in mean monthly precipitation (dark gray) and resulting uncertainty in runoff (light gray) for selected river basins (both in mm month^{-1}). The solid lines show the CRU mean monthly precipitation and the LPJmL-simulated runoff with CRU input.

2) SEASONALITY IN DISCHARGE

As expected, the basins that have a large uncertainty in the precipitation input also have a large resulting uncertainty in the estimated discharge in each season (Figs. 7a–d). However, there are some clear seasonal differences. In Europe, the relative uncertainty in summer discharge is lower than in winter, although absolute

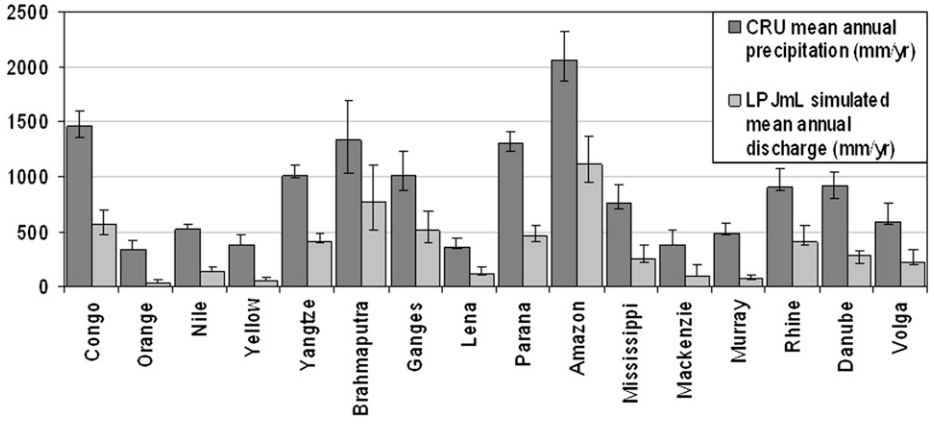

FIG. 5. CRU mean annual precipitation and resulting LPJmL-simulated discharge. Error bars represent the ranges in precipitation as derived from the seven datasets and the resulting ranges in discharge simulations.

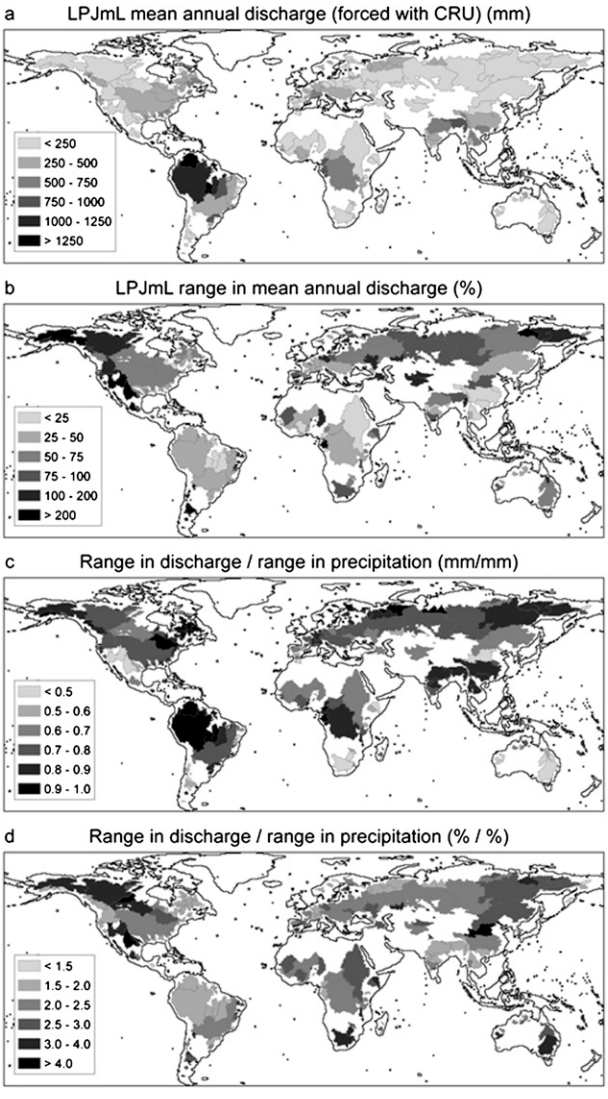

FIG. 6. (a) Mean annual discharge per basin as calculated by LPJmL based on CRU input, (b) relative range in LPJmL discharge calculations resulting from ranges in precipitation estimates, (c) absolute range in discharge over absolute range in precipitation, and (d) relative range in discharge over relative range in precipitation.

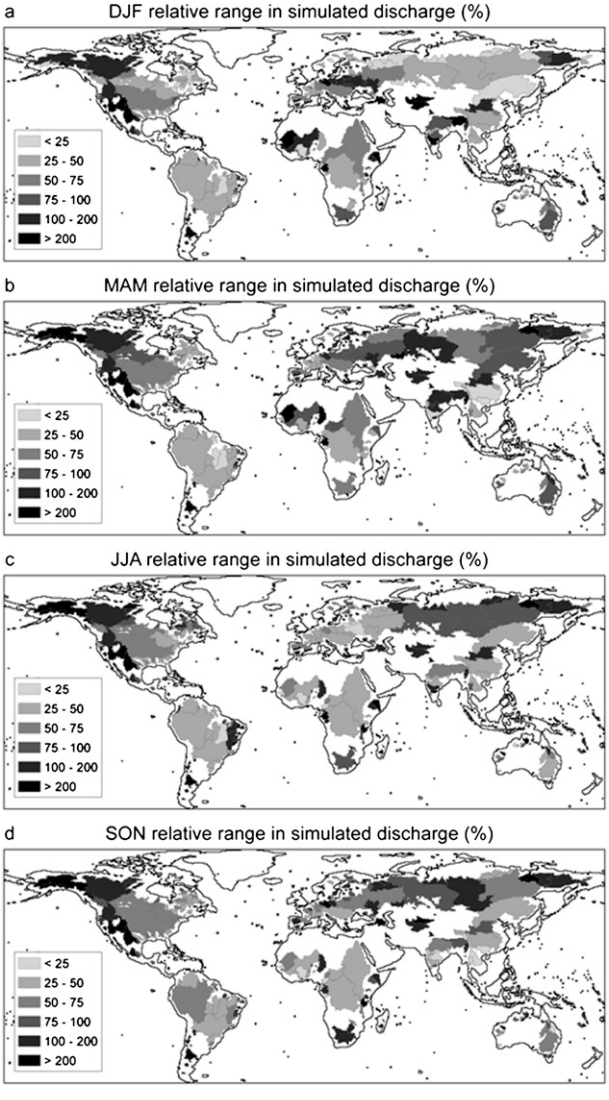

FIG. 7. Relative ranges in discharge simulations per season as percentage of the discharge simulated with CRU precipitation.

precipitation is larger in summer. In high-latitude basins the uncertainty in winter discharge is low, although the precipitation uncertainty is high in this season. The uncertainty in precipitation input leads to ranges in discharge of more than 75% in those high-latitude basins, except in winter (Fig. 7a).

In general, for all basins the precipitation uncertainty is translated into discharge uncertainty (Fig. 4). However, the largest uncertainty in precipitation and discharge do not always occur at the same time (Figs. 8a–d). In northern basins, the uncertainty in winter precipitation does not directly translate into a range in discharge. During the winter months precipitation is stored in the snowpack and only released as discharge in spring and/or summer. Large basins such as the Nile and the Amazon also show a shift of the uncertainty signal in time because of the time lag that the water needs to reach the outlet of the river.

c. *Validation with observed discharge data*

Figure 9a suggests that the LPJmL model produces too little streamflow in the high latitudes and too much streamflow in the tropical and some midlatitude basins. Assuming reliable input and validation data, it can be concluded that model calibration is necessary to compensate for the over- and underestimates, or that some processes need a better representation.

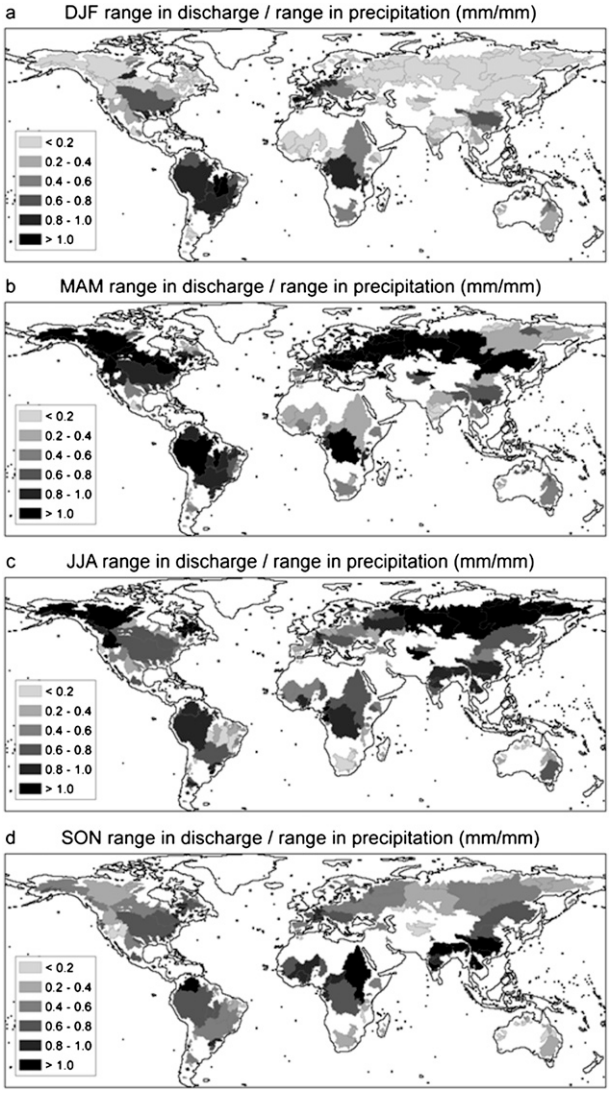

FIG. 8. Discharge uncertainty (mm) divided by precipitation uncertainty (mm) for each season.

However, as shown in the previous sections, the precipitation input is very uncertain, so, before validation and calibration of the model, the uncertainties in streamflow caused by the input uncertainties should be taken into account. When forcing the model with the minimum and maximum of precipitation for each basin, we determined that for 95 out of the 213 basins the observed discharge falls within the ranges of uncertainty of the simulated discharge. For another 23 basins, the difference between the observed and closest simulated discharge is less then 10% (Fig. 9b). For tropical basins in Africa and the Mississippi basin, the model still tends to overestimate the streamflow compared to observations, even after accounting for the uncertainty in precipitation. However, it should be noted that that these overestimations are probably caused by the fact that neither evaporation from the stream nor water extraction for irrigation are taken into account in the model run, which are both very high in those basins.

Figure 10 shows for the individual seasons that, by accounting for the precipitation uncertainty, the observed value can often be captured, whereas the model would fail more often when using a single precipitation set (CRU). However, there are some seasonal differences in that the performance is somewhat better in spring and autumn months as compared to the two solstice seasons.

d. Additional results

The model runs and analyses have been done for all basins shown in Fig. 1. For researchers with a particular interest in specific basins, these results can be consulted online. The supplemental information contains a database with information on the interannual and intra-annual variations in precipitation in each river basin as derived from the described global precipitation datasets. The resulting ranges in discharge are calculated with the LPJmL model and compared with GRDC observations, if available.

4. Discussion and conclusions

The comparison of seven global gridded precipitation datasets on a basin scale results in absolute and relative ranges in mean annual precipitation. The absolute total and relative differences in precipitation between the datasets found here at basin scale are typically lower than those found for the grid scale, as analyzed by Fekete et al. (2004). This is because a lot of the spatial differences between the datasets is averaged out when summed over a larger area. However, at basin scale the precipitation estimates still differ a lot for some basins—especially in mountainous areas where precipitation measurement errors are large and spatial interpolation is more difficult and in high latitudes where datasets not corrected for systematic wind-induced undercatch tend to underestimate the total precipitation (Adam and Lettenmaier 2003). Areas with low precipitation uncertainty typically have simpler topography, are not snow dominated, and have a dense precipitation network. Furthermore, the precipitation datasets follow the same seasonality pattern so that the main differences are in total rather than in temporal distribution of the precipitation. Exception to this pattern occurs in high-latitude basins where the uncertainty in the snow-dominated winter season is larger than in other seasons.

Our results show that the uncertainty in precipitation has a significant impact on discharge estimations. Typically, the uncertainty in precipitation propagates in larger relative uncertainty in discharge calculations.

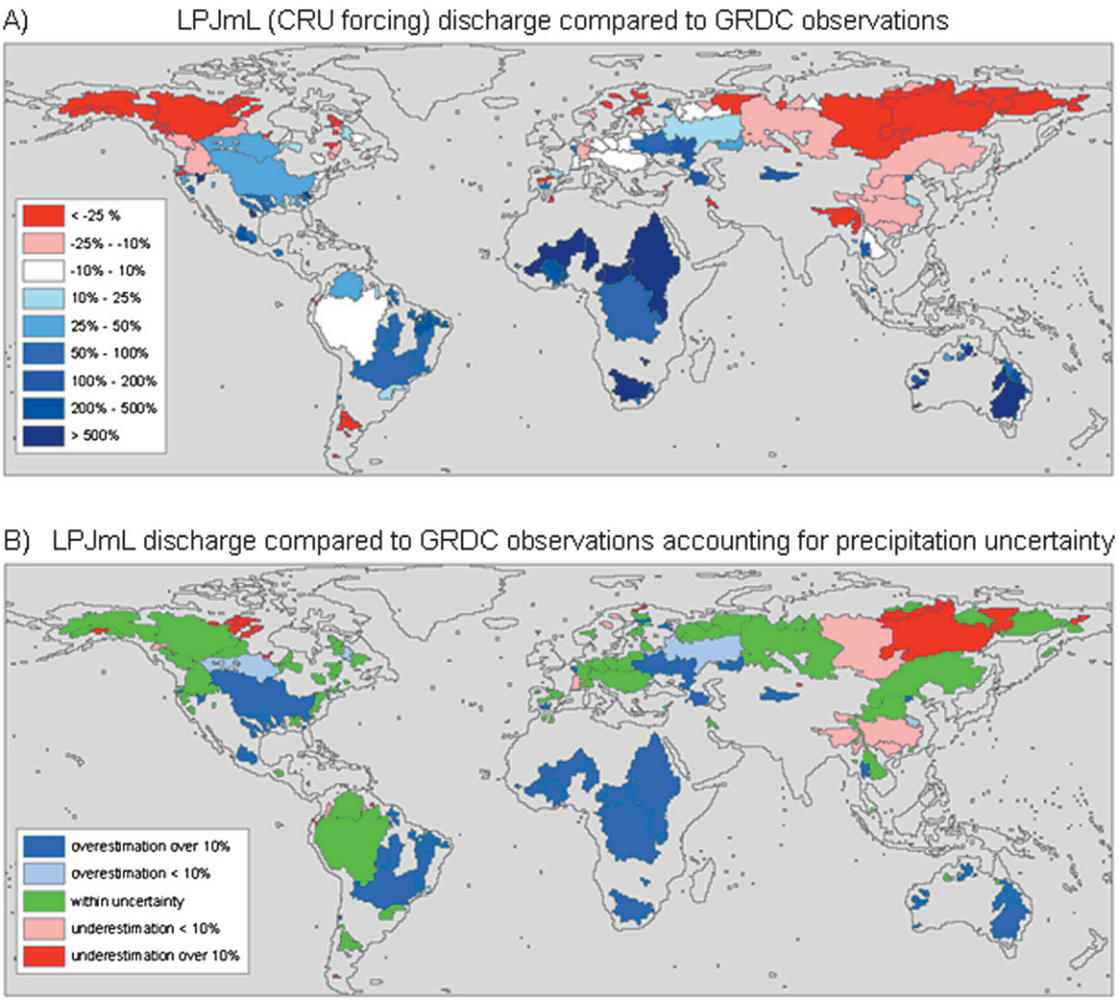

FIG. 9. (a) Differences (%) between LPJmL estimations of discharge based on CRU climatic forcing and GRDC streamflow observations. (b) Basins for which the observed discharge lies either within or outside of the simulated range under the different precipitation datasets.

Although the relative precipitation uncertainty does not change a lot during the year, the resulting discharge uncertainty does sometimes show seasonal differences. In regions where the precipitation is stored as snow in winter and released as runoff in spring, the uncertainty in winter and spring precipitation leads to a large discharge uncertainty in spring.

This quantification of the large uncertainty in discharge calculations resulting from precipitation input uncertainty is important for hydrological modelers who estimate current or future water resources, for example, studies to be conducted in the European Union Integrated Project Water and Global Change (WATCH) (available online at http://www.eu-watch.org). It makes proper validation ambiguous and calibration difficult. Most current model calibration strategies ignore this input uncertainty and estimate model parameters based on one precipitation dataset as if the precipitation was known exactly (e.g., Döll et al. 2003; Nijssen et al. 2001), possibly leading to erroneous parameter estimates and simulation results (Kavetski et al. 2002; Vrugt et al. 2005).

Discharge estimations as simulated by the LPJmL model show that including precipitation uncertainty results in a discharge uncertainty that overlaps the observed value in 95 out of 213 basins. For 23 basins the observed discharge differs less than 10% from the simulated range. Under the assumption that all precipitation datasets have the same quality and their range reflects the uncertainty, for these basins a calibration cannot improve the model results. For the other basins, where forcing the model with the different precipitation sets leads in all cases to an under- or overestimation, a calibration could improve the simulated discharge. However, it is also possible that missing processes are causing

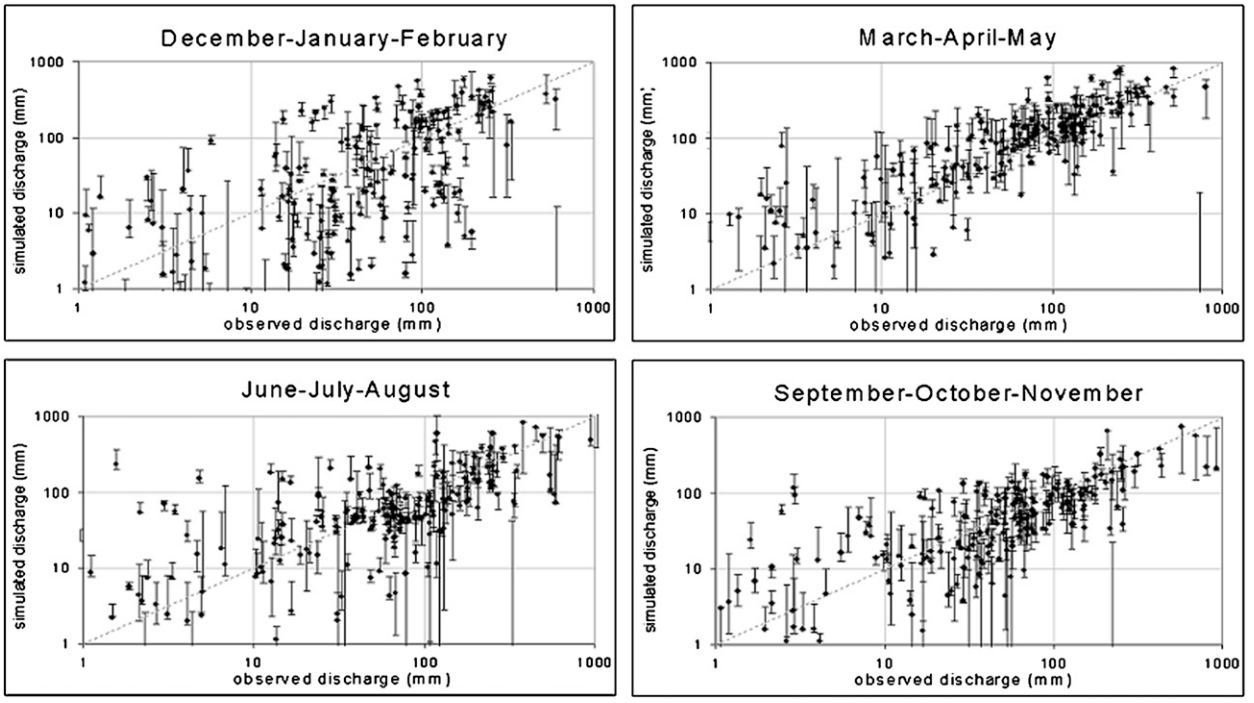

FIG. 10. Observed discharge vs range in simulated discharge for the four seasons and the 213 river basins (error bars = range; dots = values under CRU precipitation input).

the under- or overestimations. For example, for African basins the observed overestimation might be explained by the evaporative losses from stream and irrigation extractions that are not represented by the model. Another missing process that is significantly altering streamflow patterns is the operation of large reservoirs.

Because calculated discharge is to such a large extent dependent on uncertain input data, it might not be useful to calibrate a model with one particular dataset. This would give a false impression of the performance of the model. After calibration, the model seems to a large extent able to reproduce the observed discharge in river systems throughout the world. However, using a different input dataset gives other model results, thus using a different input dataset to calibrate the model could possibly lead to very different calibration parameters and, therefore, different hydrological behavior of the model.

There are three possible approaches to account for this uncertainty in global hydrological modeling (schematically illustrated in Fig. 11) to be used for future projections. Because the precipitation datasets do not differ in their representation of seasonality, these simple approaches are justified.

The first possible solution would be to calibrate the model based on multiple datasets to find the possible parameter space for the calibrated parameters. This parameter space could subsequently be used to project future water resources as a range instead of a single number. Instead of performing a calibration seven times, the precipitation coefficients in Table 2 can be used to obtain the range in precipitation estimates for each basin. The coefficients reflect the uncertainty in

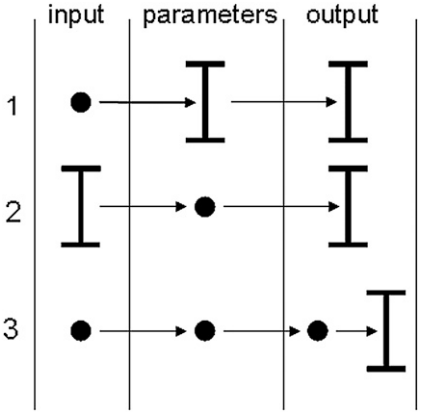

FIG. 11. Schematic presentation of three approaches to estimate the uncertainty in model output. The symbol I shows when ranges are applied. Row 1: Use of one forcing set with multiple model parameter settings to estimate the uncertainty in output. Row 2: Multiple forcing data are used with a single model to estimate the uncertainty in output (as done in this study). Row 3: The model is run with a single forcing and a single parameter set and the uncertainty is estimated afterward.

TABLE 2. Overview of the precipitation uncertainty analysis for selected basins. Results of the analysis for other basins can be found in the supplemental information (see footnote).

River basin	Station name	Mean annual precipitation 1979–99 (mm yr^{-1})					Mean annual discharge 1979–99 (m^3 s^{-1})				
		CRU	Min	Max	Min*	Max*	CRU forcing	Min	Max	Min*	Max*
Congo	Kinshasa	1454	1349	1602	0.93	1.10	65 068	54 738	79 820	0.84	1.23
Orange	Vioolsdrif	332	332	415	1.00	1.25	855	858	1 647	1.00	1.93
Nile	El Ekhsasa	523	523	565	1.00	1.08	16 708	16 708	20 076	1.00	1.20
Yellow	Huayuankou	383	383	470	1.00	1.23	1 104	1 106	2 129	1.00	1.93
Yangtze	Datong	1002	988	1096	0.99	1.09	22 465	21 782	26 871	0.97	1.20
Brahmaputra	Bahadurabad	1332	1035	1694	0.78	1.27	13 614	8 967	19 500	0.66	1.43
Ganges	Farakka	1012	873	1222	0.86	1.21	15 283	11 900	20 522	0.78	1.34
Lena	Stolb	361	349	443	0.97	1.23	8 548	7 866	13 662	0.92	1.60
Parana	Corrientes	1303	1225	1413	0.94	1.08	32 212	27 985	38 408	0.87	1.19
Amazon	Obidos	2057	1878	2329	0.91	1.13	164 630	140 931	201 771	0.86	1.23
Mississippi	Vicksburg	749	710	925	0.95	1.23	23 746	21 128	36 339	0.89	1.53
Mackenzie	Arctic Red River	387	378	512	0.98	1.33	4 863	4 590	10 030	0.94	2.06
Murray	Lock 9 upper	481	472	573	0.98	1.19	2 069	1 959	3 322	0.95	1.61
Rhine	Rees	906	870	1077	0.96	1.19	2 083	1 933	2 829	0.93	1.36
Danube	Ceatal Izmail	759	675	825	0.89	1.09	6 869	5 387	8 114	0.78	1.18
Volga	Volgograd Power Plant	587	570	750	0.97	1.28	9 261	8 730	14 740	0.94	1.59

* Values in these columns are basin-specific multiplication factors for precipitation and resulting discharge calculations. Uncertainty in precipitation and discharge can be estimated by multiplying the factors with CRU precipitation data and CRU-forced discharge.

precipitation among the seven datasets relative to CRU and can be applied to scale the CRU dataset. The parameter space can then be obtained by performing two calibrations—one on the resulting maximum dataset and one on the minimum dataset. Another way to explicitly disaggregate different sources of uncertainty in model calibration was developed by Vrugt et al. (2005) and Kavetski et al. (2006a). Kavetski et al. developed a method (Bayesian total error analysis) to account for input uncertainty in model calibration and applied this method to a hydrological model on catchment scale (Kavetski et al. 2006b). To our knowledge, no global hydrological model has been calibrated in this way, and further research is required to explore the applicability of this method to a global hydrological model.

The second option is not to calibrate but, instead, use the current model parameters and the uncertainty in precipitation to project water resources. It requires that the model parameters have physical meaning, which can be estimated from existing literature. Models that use physical parameters and have not been calibrated are MacPDM (Arnell 1999b), the water balance model (WBM) (Vörösmarty et al. 1998) and, as used here, LPJmL. To estimate the impact of precipitation uncertainty on discharge at least two model runs have to be performed, respectively with minimum and maximum estimates of precipitation. Because we have shown that the datasets show the same distribution of precipitation in time, the CRU data and precipitation coefficients derived in this study (Table 2) can be used. The minimum and maximum precipitation datasets can be obtained by multiplying the CRU values with the coefficients in Table 2 for the required basins, as done in this study.

The third option is to apply the results from the analysis presented in this paper in discharge estimations as uncertainty bands. Under the assumption that using another model for this analysis would not significantly change the results, the basin uncertainty estimations for discharge can be obtained by multiplying the model results with the coefficients in the last columns of Table 2. These coefficients can be applied to any model result to present the uncertainties in discharge resulting from precipitation uncertainty, on the condition that the model has been run, forced with CRU precipitation data. The advantage of this option is that only one model run is required, and the uncertainty in results is estimated as a postprocessing procedure.

A general conclusion of this paper is that a deterministic approach, such as it is often used in water resources research, is too simplistic. The range of uncertainty in input data has a large influence on the output and may not be neglected in the communication of results. This is even more true when modeling water resources under climate change because the uncertainty in future precipitation produced by different climate models is even larger than the uncertainty in historical data (Meehl et al. 2007). Therefore, it would be better to change to a probabilistic way of presenting results and projections of future water resources.

In this paper we have chosen not to give a quality judgment of the precipitation datasets, but to give them equal weight in the analysis. An additional study may reduce the precipitation uncertainty by eliminating the datasets known to be of less quality. However, this paper clearly shows the need for more accurate precipitation datasets to be used for forcing hydrological models.

Acknowledgments. The authors thank three anonymous reviewers for their useful comments on an earlier version of this paper. The Global Runoff Data Centre is acknowledged for the provision of global discharge data.

REFERENCES

Adam, J. C., and D. P. Lettenmaier, 2003: Adjustment of global gridded precipitation for systematic bias. *J. Geophys. Res.,* **108,** 4257, doi:10.1029/2002JD002499.

——, E. A. Clark, D. P. Lettenmaier, and E. F. Wood, 2006: Correction of global precipitation products for orographic effects. *J. Climate,* **19,** 15–38.

Adler, R. F., and Coauthors, 2003: The Version-2 Global Precipitation Climatology Project (GPCP) Monthly Precipitation Analysis (1979–present). *J. Hydrometeor.,* **4,** 1147–1167.

Alcamo, J., P. Doll, T. Henrichs, F. Kaspar, B. Lehner, T. Rosch, and S. Siebert, 2003: Development and testing of the WaterGAP 2 global model of water use and availability. *Hydrol. Sci. J.,* **48,** 317–337.

——, M. Florke, and M. Marker, 2007: Future long-term changes in global water resources driven by socio-economic and climatic changes. *Hydrol. Sci. J.,* **52,** 247–275.

Arnell, N. W., 1999a: Climate change and global water resources. *Global Environ. Change,* **9,** S31–S49.

——, 1999b: A simple water balance model for the simulation of streamflow over a large geographic domain. *J. Hydrol.,* **217,** 314–335.

——, 2003: Effects of IPCC SRES emissions scenarios on river runoff: A global perspective. *Hydrol. Earth Syst. Sci.,* **7,** 619–641.

Barnett, T. P., J. C. Adam, and D. P. Lettenmaier, 2005: Potential impacts of a warming climate on water availability in snow-dominated regions. *Nature,* **438,** 303–309.

Beck, C., J. Grieser, and B. Rudolf, 2005: A new monthly precipitation climatology for the global land areas for the period 1951 to 2000. DWD, Klimastatusbericht KSB 2004, 181–190. [Available online at http://www.ksb.dwd.de.]

Berezovskaya, S., D. Yang, and D. L. Kane, 2004: Compatibility analysis of precipitation and runoff trends over the large Siberian watersheds. *Geophys. Res. Lett.,* **31,** L21502, doi:10.1029/2004GL021277.

Bergström, S., B. Carlsson, M. Gardelin, G. Lindström, A. Pettersson, and M. Rummukainen, 2001: Climate change impacts on runoff in Sweden—Assessments by global climate models, dynamical downscaling and hydrological modelling. *Climate Res.,* **16,** 101–112.

Bondeau, A., and Coauthors, 2007: Modelling the role of agriculture for the 20th century global terrestrial carbon balance. *Global Change Biol.,* **13,** 679–706.

Climate Prediction Center, cited 2008: CPC Merged Analysis of Precipitation (CMAP). Climate Prediction Center. [Available online at http://www.cpc.noaa.gov/products/global_precip/html/wpage.cmap.html.]

CSD, 1997: Comprehensive assessment of the freshwater resources of the world. Commission on Sustainable Development, Rep. of the Secretary-General E/CN.17/1997/9, 52 pp.

Döll, P., and B. Lehner, 2002: Validation of a new global 30-min drainage direction map. *J. Hydrol.,* **258,** 214–231.

——, F. Kaspar, and B. Lehner, 2003: A global hydrological model for deriving water availability indicators: Model tuning and validation. *J. Hydrol.,* **270,** 105–134.

Fekete, B. M., C. J. Vörösmarty, and W. Grabs, 2000: Global composite runoff fields based on observed river discharge and simulated water balances. Global Runoff Data Centre Rep. 22, 39 pp.

——, ——, and ——, 2002: High-resolution fields of global runoff combining observed river discharge and simulated water balances. *Global Biogeochem. Cycles,* **16,** 1042, doi:10.1029/1999GB001254.

——, ——, J. O. Roads, and C. J. Willmott, 2004: Uncertainties in precipitation and their impacts on runoff estimates. *J. Climate,* **17,** 294–304.

Gerten, D., S. Schaphoff, U. Haberlandt, W. Lucht, and S. Sitch, 2004: Terrestrial vegetation and water balance—Hydrological evaluation of a dynamic global vegetation model. *J. Hydrol.,* **286,** 249–270.

Global Runoff Data Centre, cited 2007: The GRDC—The worldwide repository of river discharge data and associated metadata. [Available online at http://grdc.bafg.de.]

Huffman, G. J., and Coauthors, 1997: The Global Precipitation Climatology Project (GPCP) combined precipitation dataset. *Bull. Amer. Meteor. Soc.,* **78,** 5–20.

Kabat, P., and Coauthors, 2004: *Vegetation, Water, Humans and the Climate: A New Perspective on an Interactive System*. Global Change: The IGBP Series, Vol. 24, Springer, 566 pp.

Kavetski, D., S. W. Franks, and G. Kuczera, 2002: Confronting input uncertainty in environmental modelling. *Calibration of Watershed Models*, Q. Duan, et al., Eds., 49–68.

——, G. Kuczera, and S. W. Franks, 2006a: Bayesian analysis of input uncertainty in hydrological modeling: 1. Theory. *Water Resour. Res.,* **42,** W03407, doi:10.1029/2005WR004368.

——, ——, and ——, 2006b: Bayesian analysis of input uncertainty in hydrological modeling: 2. Application. *Water Resour. Res.,* **42,** W03408, doi:10.1029/2005WR004376.

Kundzewicz, Z. W., and Coauthors, 2007: Freshwater resources and their management. *Climate Change 2007: Impacts, Adaptation and Vulnerability*, M. L. Parry et al., Eds., Cambridge University Press, 173–210.

Legates, D. R., 1987: *A Climatology of Global Precipitation*. Publications in Climatology, Vol. 40, Laboratory of Climatology, 91 pp.

——, and C. J. Willmott, 1990: Mean seasonal and spatial variability in gauge-corrected, global precipitation. *Int. J. Climatol.,* **10,** 111–127.

Matsuura, K., and C. J. Willmott, cited 2007: Terrestrial Precipitation: 1900-2006 Gridded Monthly Time Series (version 1.01). Center for Climatic Research, Department of Geography, University of Delaware. [Available online at http://climate.geog.udel.edu/~climate/.]

Meehl, G. A., and Coauthors, 2007: Global climate change projections. *Climate Change 2007: The Physical Science Basis,* S. Solomon et al., Eds., Cambridge University Press, 747–846.

Milly, P. C. D., K. A. Dunne, and A. V. Vecchia, 2005: Global pattern of trends in streamflow and water availability in a changing climate. *Nature,* **438,** 347–350.

Mitchell, T. D., and P. D. Jones, 2005: An improved method of constructing a database of monthly climate observations and associated high-resolution grids. *Int. J. Climatol.,* **25,** 693–712.

New, M., M. Hulme, and P. Jones, 1999: Representing twentieth-century space–time climate variability. Part I: Development of a 1961–90 mean monthly terrestrial climatology. *J. Climate,* **12,** 829–856.

——, ——, and ——, 2000: Representing twentieth-century space–time climate variability. Part II: Development of 1901–96 monthly grids of terrestrial surface climate. *J. Climate,* **13,** 2217–2238.

Nijssen, B., G. M. O'Donnell, D. P. Lettenmaier, D. Lohmann, and E. F. Wood, 2001: Predicting the discharge of global rivers. *J. Climate,* **14,** 3307–3323.

Oki, T., Y. Agata, S. Kanae, T. Saruhashi, D. Yang, and K. Musiake, 2001: Global assessment of current water resources using total runoff integrating pathways. *Hydrol. Sci. J.,* **46,** 983–995.

Österle, H., F. W. Gerstengarbe, and P. C. Werner, 2003: Homogenisierung und Aktualisierung des Klimadatensatzes des Climate Research Unit, University of East Anglia, Norwich. Preprints, *Sixth German Climate Conf.: Climate Variability,* Potsdam, Germany, Alfred-Wegener Foundation, 326–329.

Pavelsky, T. M., and L. C. Smith, 2006: Intercomparison of four global precipitation data sets and their correlation with increased Eurasian river discharge to the Arctic Ocean. *J. Geophys. Res.,* **111,** D21112, doi:10.1029/2006JD007230.

Rost, S., D. Gerten, A. Bondeau, W. Lucht, J. Rohwer, and S. Schaphoff, 2008: Agricultural green and blue water consumption and its influence on the global water system. *Water Resour. Res.,* **44,** W09405, doi:10.1029/2007WR006331.

Sitch, S., and Coauthors, 2003: Evaluation of ecosystem dynamics, plant geography and terrestrial carbon cycling in the LPJ dynamic global vegetation model. *Global Change Biol.,* **9,** 161–185.

Tian, X., A. Dai, D. Yang, and Z. Xie, 2007: Effects of precipitation-bias corrections on surface hydrology over northern latitudes. *J. Geophys. Res.,* **112,** D14101, doi:10.1029/2007JD008420.

USGS, 2000: HYDRO1k elevation derivative database. U.S. Geological Survey. [Available online at http://eros.usgs.gov/products/elevation/gtopo30/hydro/index.html.]

Voisin, N., A. W. Wood, and D. P. Lettenmaier, 2008: Evaluation of precipitation products for global hydrological prediction. *J. Hydrometeor.,* **9,** 388–407.

Vörösmarty, C. J., C. A. Federer, and A. L. Schloss, 1998: Potential evaporation functions compared on US watersheds: Possible implications for global-scale water balance and terrestrial ecosystem modeling. *J. Hydrol.,* **207,** 147–169.

——, P. Green, J. Salisbury, and R. B. Lammers, 2000a: Global water resources: Vulnerability from climate change and population growth. *Science,* **289,** 284–288.

——, B. M. Fekete, M. Meybeck, and R. B. Lammers, 2000b: Global system of rivers: Its role in organizing continental land mass and defining land-to-ocean linkages. *Global Biogeochem. Cycles,* **14,** 599–621.

Vrugt, J. A., C. G. H. Diks, H. V. Gupta, W. Bouten, and J. M. Verstraten, 2005: Improved treatment of uncertainty in hydrologic modeling: Combining the strengths of global optimization and data assimilation. *Water Resour. Res.,* **41,** W01017, doi:10.1029/2004WR003059.

Willmott, C. J., and K. Matsuura, 2001: Terrestrial air temperature and precipitation: Monthly and annual time series (1950–1999) (version 1.02). Center for Climate Research, University of Delaware. [Available online at http://climate.geog.udel.edu/~climate/.]

World Water Council, 2000: A water secure world: Vision for water, life and the environment. World Water Vision: Commission Rep., 70 pp.

Xie, P. P., and P. A. Arkin, 1997: Global precipitation: A 17-year monthly analysis based on gauge observations, satellite estimates, and numerical model outputs. *Bull. Amer. Meteor. Soc.,* **78,** 2539–2558.